Eur. J. Biochem. 235, 310–316 (1996)

Inhibitory properties of separate recombinant Kunitz-type-protease-inhibitor domains from tissue-factor-pathway inhibitor

Lars C. PETERSEN, Søren E. BJØRN, Ole H. OLSEN, Ole NORDFANG, Funny NORRIS and Kjeld NORRIS

Health Care Discovery, Vessel Wall Biology, Novo Nordisk A/S, Gentofte, Denmark

(Received 24 August/19 October 1995) – EJB 95 1396/3

Tissue-factor-pathway inhibitor (TFPI) is a multivalent inhibitor with three tandemly arranged Kunitz-type-protease-inhibitor (KPI) domains. Previous studies [Girard, Y. J., Warren, L. A., Novotny, W. F., Likert, K. M., Brown, S. G., Miletich, J. P. & Broze, G. J. (1989) *Nature 338*, 518–520] by means of site-directed mutagenesis indicated that KPI domain 1 interacts with factor VII_a, that KPI domain 2 interacts with factor X_a, and that KPI domain 3 is apparently without inhibitory function. To elucidate the reaction mechanism of this complex inhibitor, we followed a different approach and studied the inhibitory properties of fragments of TFPI obtained by expression in yeast. Results obtained with TFPI-(1–161)-peptide and separate recombinant TFPI-KPI domains 1, 2 and 3 showed that KPI domain 1 inhibited factor VII_a/tissue factor (K_i = 250 nM), KPI domain 2 inhibited factor X_a (K_i = 90 nM), and that KPI domain 3 was without detectable inhibitory function. Studies with separate KPI domains also showed that KPI domain 2 was mainly responsible for inhibition of trypsin (K_i = 0.1 nM) and chymotrypsin (K_i = 0.75 nM), whereas KPI domain 1 inhibited plasmin (K_i = 26 nM) and cathepsin G (K_i = 200 nM). The structural basis for the interaction between serine proteases and KPI domains is discussed in terms of putative three-dimensional models of the proteins derived by comparative molecular-modelling methods. Studies of factor X_a inhibition by intact TFPI ($K_i \approx 0.02$ nM) suggested that regions other than the contact area of the KPI domain, interacted strongly with factor X_a. Secondary-site interactions were crucial for TFPI inhibition of factor X_a but was of little or no importance for its inhibition of trypsin.

Keywords: tissue-factor-pathway inhibitor; Kunitz-type protease inhibitor; factor X; factor VII.

Injury and vascular-wall damage causes exposure of tissue factor (TF) to the blood stream, and the appearance of this cell-bound receptor results in dramatic upregulation of the coagulation cascade (see [1] for review). The initial event in this process is binding of factor VII to TF and its conversion to active factor VII_a by factor IX_a or X_a [2]. Auto-activation of factor VII by factor VII_a may also play a significant role [3, 4]. TF-bound factor VII_a is also capable of activating factors X and IX [5, 6]. This reciprocal zymogen-activation cycle is central to the triggering of the TF-dependent-coagulation pathway, and once initiated the cycle generates factor X_a which converts prothrombin to thrombin. Ultimately this leads to fibrin-clot formation.

Initiation of the TF pathway is under strict control by an inhibitor [7–9] now designated as tissue-factor-pathway inhibitor (TFPI). Based on the primary structure predicted from cDNA sequence analysis [10] and expression in transfected mammalian-cell systems [11, 12] detailed knowledge about the inhibitor has been obtained [8, 13]. TFPI is a multivalent inhibitor (molecular mass of 40 kDa) with three tandemly arranged Kunitz-type-protease-inhibitor (KPI) domains [10], each of which may provide a putative contact region for the active site of a protease. The specificity of the inhibitor domains has been studied by site-directed mutagenesis [11]. The results showed that the first KPI domain interacts with the active site of factor VII_a, and that the second KPI domain interacts with the active site of factor X_a. No inhibitory function could be attributed to the third KPI domain. A model involving a quaternary factor X_a · factor VII_a · TF complex was proposed in order to explain that an efficient inhibition of factor VII_a · TF was only observed in the presence of factor X_a [11]. This complex inhibition pattern suggested that in addition to the direct interactions between proteases and the KPI domains, other regions of TFPI might be involved in its

Correspondence to L. C. Petersen, Leucocyte Research, Vessel Wall Biology, Novo Nordisk A/S, Hagedornsvej 1, DK-2820 Gentofte, Denmark

Fax: +45 4438092.

Abbreviations. TFPI, tissue-factor-pathway inhibitor; KPI, Kunitz-type protease inhibitor; TF, tissue factor; BPTI, bovine pancreatic trypsin inhibitor; Val-Leu-Lys-NH-Np, D-valyl-L-leucyl-L-lysine *p*-nitroanilide; MeO-Suc-Arg-Pro-Tyr-NH-Np, methoxy succinyl-L-arginyl-L-prolyl-L-tyrosine *p*-nitroanilide; Val-Leu-Arg-NH-Np, D-valyl-L-leucyl-L-arginine *p*-nitroanilide; Glp-Gly-Arg-NH-Np, 5-oxoprolyl-glycyl-L-arginine *p*-nitroanilide; Ile-Pro-Arg-NH-Np, D-isoleucyl-L-prolyl-L-arginine *p*-nitroanilide; Cbz-D-Arg-Gly-Arg-NH-Np, *N*-α-benzyloxycarbonyl-D-arginyl-glycyl-L-arginine *p*-nitroanilide; MeO-CO-cHxo-Gly-Arg-NH-Np, methoxycarbonyl-D-cyclohexanoyl-glycyl-L-arginine *p*-nitroanilide; MeO-Suc-Ala-Ala-Pro-Val-NH-Np, methoxysuccinyl-L-alanyl-L-alanyl-L-prolyl-L-valine *p*-nitroanilide; Suc-Ala-Ala-Pro-Phe-NH-Np, succinyl-L-alanyl-L-prolyl-L-phenyl *p*-nitroanilide; PDMS, plasmadesorption mass spectrometry.

Enzymes. Trypsin, porcine (EC 3.4.21.4); chymotrypsin, bovine (EC 3.4.21.1); leukocyte elastase, human (EC 3.4.21.37); cathepsin G, human (EC 3.4.21.20); coagulation factor X_a, human (EC 3.4.21.6); coagulation factor VII_a, human (EC 3.4.21.21).

function. Subsequent studies have revealed that the anticoagulant activity of TFPI is significantly reduced upon removal of a C-terminal fragment of the molecule by proteolytic cleavage [14, 15], and it has been shown [16, 17] that specific cleavage of the Thr87-Thr88 bond by leukocyte elastase has a dramatic effect on the inhibitory properties of TFPI. This cleavage separates KPI domain 1 from the rest of the molecule, and this event not only interferes with the inhibition of factor VII_a/TF, but also abrogates the TFPI-mediated inhibition of factor X_a. The present study investigates the properties of this multivalent inhibitor and describes the expression, purification and characterisation of separate KPI domains and selected fragments of TFPI.

MATERIALS AND METHODS

Substrates. Chromogenic substrates, D-valyl-L-leucyl-L-lysine *p*-nitroanilide (Val-Leu-Lys-NH-Np); methoxy succinyl-L-arginyl-L-prolyl-L-tyrosine *p*-nitroanilide (MeO-Suc-Arg-Pro-Tyr-NH-Np); D-valyl-L-leucyl-L-arginine *p*-nitroanilide (Val-Leu-Arg-NH-Np); 5-oxoprolyl-glycyl-L-arginine *p*-nitroanilide (Glp-Gly-Arg-NH-Np); D-isoleucyl-L-prolyl-L-arginine *p*-nitroanilide (Ile-Pro-Arg-NH-Np) and *N*-α-benzyloxycarbonyl-D-arginyl-glycyl-L-arginine *p*-nitroanilide (Cbz-D-Arg-Gly-Arg-NH-Np) were purchased from Chromogenix, methoxycarbonyl-D-cyclohexanoyl-glycyl-L-arginine *p*-nitroanilide (MeO-CO-cHxo-Gly-Arg-NH-Np) was from NycoMed, and methoxysuccinyl-L-alanyl-L-alanyl-L-prolyl-L-valine *p*-nitroanilide (MeO-Suc-Ala-Ala-Pro-Val-NH-Np) and succinyl-L-alanyl-L-prolyl-L-phenyl *p*-nitroanilide (Suc-Ala-Ala-Pro-Phe-NH-Np) were from Sigma.

Proteases. Recombinant human factor VII_a, porcine trypsin and chymotrypsin were from Novo Nordisk. Human leukocyte elastase and cathepsin G were purified according to the procedure described by Baugh and Travis [18]. Human factor X_a was a generous gift from Dr W. Kisiel (Albuquerque, NM).

TFPI and C-terminally truncated derivatives expressed in BHK cells. Recombinant TFPI was purified from the culture media of transfected BHK cells and initially purified as a heterogenous mixture of intact and C-terminally degraded TFPI by heparin-affinity and ion-exchange chromatography steps [12]. The C-terminally degraded form represents a heterogeneous mixture of proteins which contain at least residues 1−247 and is designated as TFPI-(1−247)-peptide. Intact TFPI [TFPI-(1−276)] was separated from C-terminally degraded TFPI by chromatography on a Mono S column from Pharmacia as previously described [14].

TFPI-(1–161)-peptide expressed in yeast. A TFPI derivative containing KPI domains 1 and 2 [TFPI-(1−161)-peptide] was expressed as secreted protein in yeast [19, 20]. This protein is heterogenously glycosylated with a high-mannose glycan containing 13−17 mannose residues. The protein was purified using ion-exchange and gel-permeation techniques [20].

Expression of TFPI-(22–79)-peptide (KPI domain 1), TFPI-(93–150)-peptide (KPI domain 2) and TFPI-(185–242)-peptide (KPI domain 3) in yeast. Individual KPI domains of TFPI were cloned by PCR with a mammalian expression vector encoding full-length TFPI [12] as a template. The PCR primers GCTGAGAGATTGGAGAAGAGAATGCATTCATTTTGTGC and TAATCCTTCTAGATTAATCTCTTGTACACAT [TFPI-(22−150)-peptide], GCTGAGAGATTGGAGAAGAGAAAGCCAGATTTCTGCTT and CTGGAATCTAGATTAACCATCTTCACAAATGTT [TFPI-(93−150)-peptide], and GCTGAGAGATTGGAGAAGAGAGGTCCCTCATGGTGTCT and GATATTCTTCTAGATTAACCTTTTTTACATGCCCT [TFPI-(185−242)-peptide] were used as described for the PCR cloning of the Alzheimer-amyloid-protein-precursor-homolog KPI domain [21]. Fusion of the PCR products in-frame to a hybrid yeast-leader sequence, construction of the expression vector, transformation of yeast strain MT-663 and fermentation were essentially as described [21]. At the end of the fermentation the culture was adjusted to pH 3.0 by addition of 18 M H_3PO_4 and the supernatant isolated after centrifugation at 1000 *g* for 20 min.

Purification of KPI domain 1. The supernatant described above was applied to an S-Sepharose Fast Flow column (2.6 cm×3.6 cm; Pharmacia) equilibrated with 50 mM formic acid, pH 3.7. After washing with equilibration buffer, the antitrypsin activity was eluted with 40 ml 1 M NaCl. Desalting was performed on a Sephadex G-25 column (2.6 cm×34 cm; Pharmacia) equilibrated in 0.1% NH_4HCO_3, pH 7.9. KPI domain 1 was eluted with the same buffer. After concentration by vacuum centrifugation and adjustment to pH 3.0, further purification was performed on a Mono S column (0.5 cm×5 cm; Pharmacia) by gradient elution over 25 min at 1 ml/min from 0 to 0.75 M NaCl in 50 mM formic acid, pH 3.7. Final purification of KPI domain 1 was performed by reverse-phase HPLC on a Vydac C4 column (1.0 cm×25 cm; The Separation Group) by gradient elution over 60 min at 4 ml/min from 15% to 60% acetonitrile in 0.1% trifluoroacetic acid. KPI domain 1 eluted in about 30% acetonitrile and the purified product was lyophilized and redissolved in water. Samples were analyzed by amino acid sequencing and plasma-desorption mass spectroscopy (PDMS) (observed molecular mass of 6854 Da; calculated molecular mass of 6854 Da). The overall yield of KPI domain 1 was low; only 40 mg of pure inhibitor was isolated from 2200 ml yeast-fermentation supernatant.

Purification of KPI domain 2. S-Sepharose chromatography and desalting on Sephadex G-25 was performed as described above. Further purification was performed on a Mono S column (1.0 cm×10 cm) by gradient elution over 30 min at 4 ml/min from 0 to 0.3 M NaCl in 20 mM Tris/HCl, pH 8.5. N-glycosylated and non-glycosylated KPI domain 2 eluted at 0.1 M and 0.15 M NaCl, respectively. Final purification of non-glycosylated KPI domain 2 was performed by reverse-phase HPLC on a Vydac C4 column by gradient elution over 25 min at 4 ml/min from 5% to 55% acetonitrile in 0.1% trifluoroacetic acid. KPI domain 2 eluted in 35% acetonitrile. The purified product was lyophilized and redissolved in water at approximately 200 nM. Samples were analyzed for amino acid composition, and by PDMS (observed molecular mass of 6841 Da; calculated molcular mass of 6841 Da).

Purification of KPI domain 3. The supernatant was applied to a S-Sepharose Fast Flow column equilibrated with 50 mM formic acid, pH 3.7. After washing with equilibration buffer, the protein was eluted with 1 M NaCl. Desalting was performed on a PD 10 column (Pharmacia) equilibrated in 50 mM formic acid, pH 3.7. KPI domain 3 was eluted with the same buffer. Further purification was obtained on a Mono S column by gradient elution over 25 min at 1 ml/min from 0 to 0.75 M NaCl in 50 mM formic acid, pH 3.7. Final purification of KPI domain 3 was performed by reverse-phase HPLC on a Vydac C4 column by gradient elution over 25 min at 1.5 ml/min from 5% to 55% acetonitrile in 0.1% trifluoroacetic acid. The purified product was lyophilized and redissolved in water. Aliquot samples were analyzed by amino-acid sequencing and PDMS (observed molecular mass of 6493 Da; calculated molecular mass of 6491 Da).

Inhibition assays and kinetics. Kinetic measurements were performed in 50 mM Tris/HCl, 100 mM NaCl, pH 7.4 at 25°C in 96-well microtiter plates. The change in absorbance at 405 nm was monitored by means of an SLT ELISA Reader. The apparent inhibition constant K_i' was determined from measurements ob-

tained under steady-state conditions by means of a non-linear data-analysis program Enzfitter® (Biosoft). Where indicated the data sets for inhibition of trypsin and factor X_a were analyzed in terms of the equation for a tight-binding inhibitor (Eq. 1):

$$v_i = \frac{v_0}{2}\left[\sqrt{(K_i' + [I]_0 + [E]_0)^2 - 4[I]_0[E]_0} - (K_i' + [I]_0 + [E]_0)\right] \quad (1)$$

where v_i and v_0 are inhibited and un inhibited rates, respectively, and $[I]_0$ and $[E]_0$ are the total concentrations of enzyme and inhibitor, respectively. Where $K_i \gg [E]_0$ inhibition data were analyzed according to Eq. (2):

$$v_i = v_0 \frac{K_i'}{K_i' + [I]_0}. \quad (2)$$

Assuming inhibition is competitive the true inhibition constant K_i was calculated according to Eq. (3):

$$K_i = K_i' \frac{K_m}{[S] + K_m}. \quad (3)$$

The data for the transient-inhibition experiments were analyzed according to Eq. (4):

$$A_t = A_{amp}(1 - e^{-k_{obs}t}) + k_0 t \quad (4)$$

where A_t is the absorbance at 405 nm at time t, k_{obs} is the apparent first-order constant for transition to steady-state, k_0 is a constant describing the steady-state rate of product generation, and A_{amp} is the amplitude of the absorbance change obtained by back extrapolation to $t = 0$ of the steady-state-product-generation curve [22].

Molecular modelling. The molecular-structure models used for analysis of the inhibition measurements were obtained either from X-ray studies or produced by computer modelling by a homology-based strategy. Structure analysis and molecular modelling were conducted on Silicon Graphics systems using the modelling-program package QUANTA (Molecular Simulation Inc.) Model building of TFPI-KPI domain 1 is mainly based on the structure of the KPI domain from the Alzheimer-amyloid-protein precursor [23] (Brookhaven entry 1app). The model of TFPI-KPI domain 2 was obtained from X-ray diffraction studies [24]. Model building of TFPI-KPI domain 3 is based on the structure of BPTI [25] (Brookhaven entry 4pti). The overall three-dimensional structures of the scaffold of KPI domains are usually very similar, and the structure of BPTI may therefore serve as a general model. Recent X-ray studies, however, have revealed that the structure of the reactive loop in some KPI domains may differ significantly from that of BPTI. Thus the P′ side of this loop (residues 16–19) in TFPI domain 2 [24] and the P′ side of the loop of the KPI domain of the α3 chain of type VI collagen [26], have been dramatically changed. This is caused by the interaction of the aromatic rings in position 17 with a hydrophobic pocket consisting of the side chains of residues 11 and 34, which causes the backbone carbonyl of residue 16 and the backbone nitrogen of residue 17 to rotate almost 180°. Further, these X-ray data and recent NMR studies of an amino-acid-substitution analog of BPTI [27] have shown that the Cys14-Cys38 disulphide bridge bond on the P side may differ in chirality from the conformation found in BPTI. These observations have been considered in the models of TFPI-KPI domains 1 and 3.

The X-ray structures of trypsin and chymotrypsin are known. The structures of factor X, factor VII and cathepsin G have been deduced from that of chymotrypsin [28] (Brookhaven entry 5cha) and rat mast cell protease [29] (Brookhaven entry 3rp2).

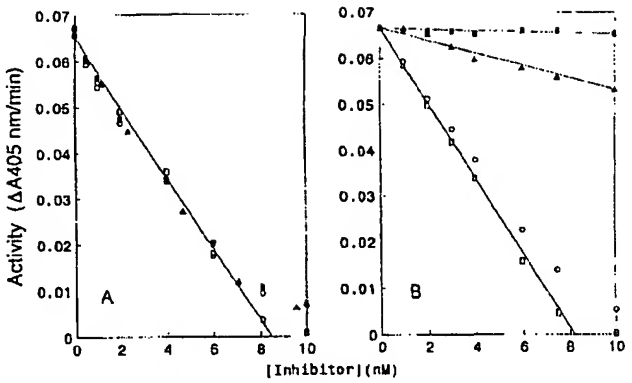

Fig. 1. Trypsin inhibition by TFPI derivatives. (A) Full-length TFPI, (○); TFPI-(1–247)-peptide, (▲); TFPI-(1–161)-peptide, (■). (B) KPI domain 1, (▲); KPI domain 2, (○); KPI domain 3, (■). Inhibition by BPTI (□) is shown for comparison. Trypsin (8.2 nM) was incubated with various concentrations of BPTI or TFPI derivatives for 15 min. Substrate (0.5 mM Val-Leu-Lys-NH-Np) was then added and residual activity measured.

To gain a detailed understanding of the structural features that govern the interaction between KPI domains and serine proteases, models have been obtained of the inhibitors inserted into the substrate-binding clefts of the proteases. The BPTI · trypsin complex [30] (Brookhaven entry 2tpi) has been used as a guide for this modelling.

RESULTS

Inhibition of trypsin. Full-length TFPI [TFPI-(1–276)], C-terminally truncated TFPI [TFPI-(1–247)-peptide], and the N-terminal two domains of TFPI [TFPI-(1–161)-peptide] inhibited trypsin with high affinity (Fig. 1A). Assuming that each of the three derivatives binds trypsin in a 1:1 stoichiometry, this property can be used to determine an accurate value for the functional concentration of these inhibitors.

TFPI consists of three KPI domains. At least two domains, domains 1 and 2, have been shown to be functional inhibitory domains [11, 31]. The TFPI molecule may be bi-functional and thus inhibit more than one molecule of trypsin. To test this hypothesis, the inhibition of trypsin by separate KPI domains was investigated (Fig. 1B). KPI domain 3 was non-inhibitory, KPI domain 1 inhibited trypsin weakly (K_i = 1 μM), and KPI domain 2 inhibited trypsin with an affinity comparable to that of multi-domain TFPI derivatives.

The inhibition of trypsin by TFPI, TFPI fragments and KPI domains was measured in separate experiments. The results obtained with full-length TFPI, TFPI-(1–247)-peptide, and TFPI-(1–161)-peptide were analyzed in terms of tight-binding inhibition as described in Materials and Methods and the K_i values are listed in Table 1.

Analysis of the reaction between TFPI and trypsin supported the notion that the inhibition of this protease involved exclusively the interaction between TFPI-KPI domain 2 and the protease. Fig. 2 shows that the profile of inhibition of trypsin by TFPI-(1–247)-peptide was indistinguisable from inhibition by the separate TFPI-(22–79)-peptide domain. Similar results (data not shown) were obtained with full-length TFPI and TFPI-(1–161)-peptide. The transient inhibition of trypsin by BPTI is shown for comparison (Fig. 2). Binding of TFPI to trypsin was 30-fold faster ($k_i = 1.7\times10^6$ M^{-1} s^{-1}) than binding of BPTI ($k_i = 0.51\times10^6$ M^{-1} s^{-1}). The latter rate constant is in excellent

Table 1. Inhibition of various serine proteases by TFPI derivatives. K_i values were calculated from apparent K_i (K_i') values according to (Eqn. 3). Measurements were made in 50 mM Tris/HCl, 100 mM NaCl, 0.01% Tween 80, pH 7.4, 25°C. Factor VIIa (10 nM) and TF (16 nM) were assayed with 0.6 mM Ile-Pro-Arg-NH-Np ($K_m \gg [S]$); factor Xa (1 nM) with 0.3 mM MeOCO-cHxo-Gly-Arg-NH-Np (K_m = 0.3 mM); trypsin (8 nM) with 0.6 mM Val-Leu-Lys-NH-Np (K_m = 0.31 mM); chymotrypsin (2.5 nM) with 0.6 mM MeO-Suc-Arg-Pro-Tyr-NH-Np (K_m = 0.06 mM); cathepsin G (10 nM) with 0.6 mM Suc-Ala-Ala-Pro-Phe-NH-Np (K_m = 2.9 mM); and plasmin (10 nM) with 0.6 mM Val-Leu-Lys-NH-Np (K_m = 0.21 mM). n.d., not determined; −, no inhibition at 1×10^{-6} M.

Peptide	K_i values					
	Factor VII$_a$/TF	factor X$_a$	trypsin	chymo-trypsin	cathepsin G	plasmin
	nM					
TFPI-(22−79), KPI-1	250	−	12	150	200	26
TFPI-(93−150), KPI-2	1100	90	0.1	0.75	−	~500
TFPI-(185−242), KPI-3	−	−	−	−	−	−
TFPI-(1−161)	120	0.15	0.15	0.56	58	24
TFPI-(1−247)	120	0.07	0.12	0.54	n.d.	n.d.
TFPI-(1−276)	120	≈ 0.02	0.12	0.62	n.d.	15

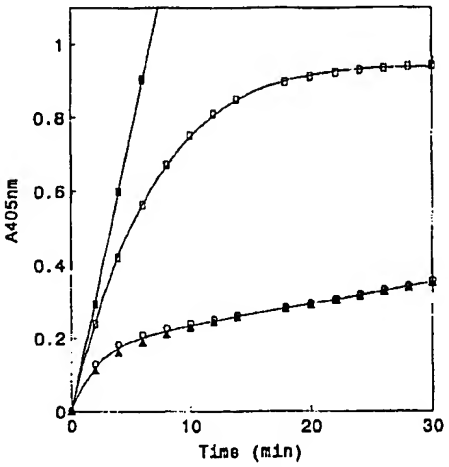

Fig. 2. Transient inhibition of trypsin by TFPI derivatives. Trypsin (2.5 nM) was added to a mixture of 20 nM inhibitor and 0.6 mM Glp-Gly-Arg-NH-Np. The generation of *p*-nitroaniline was followed at 405 nm. KPI domain 2, (○); full-length TFPI, (▲). The trypsin activity in the absence of inhibitor (■) and the transient inhibition by 20 nM BPTI (□) are shown for comparison.

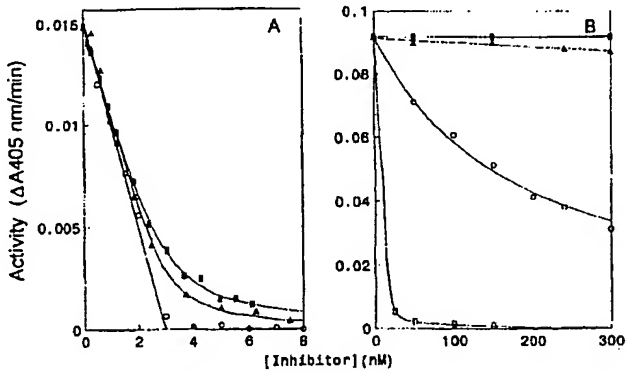

Fig. 3. Factor X$_a$ inhibition by TFPI derivatives. (A) Full-length TFPI, (○); TFPI-(1−247)-peptide, (▲); TFPI-(1−161)-peptide, (■). (B) TFPI-(1−161)-peptide, (□); KPI domain 1, (▲); KPI domain 2, (○); KPI domain 3, (■). Factor X$_a$ [2.5 nM in (A), 3 nM in (B)] was incubated with various concentrations of TFPI derivatives for 15 min. Substrate [0.5 mM Glp-Gly-Arg-NH-Np in (A), 0.375 mM MeO-CO-cHxo-Gly-Arg-NH-Np in (B)] was then added and residual activity measured.

agreement with the k_i value of 0.59×10^6 M^{-1} s^{-1} obtained by Zhou et al. [32]. However, Fig. 2 also shows that the extent of inhibition of trypsin by BPTI was greater than by TFPI.

Inhibition of chymotrypsin, plasmin, cathepsin G and human leukocyte elastase. Previous experiments with TFPI have shown that it was an inhibitor of chymotrypsin and plasmin [33]. TFPI has also been shown to inhibit cathepsin G and leukocyte elastase [17], although with low affinity. The results obtained on inhibition of these proteases are summarized in Table 1. They suggest that KPI domain 2 is primarily responsible for the interaction with chymotrypsin, whereas KPI domain 1 accounts for the inhibition of plasmin, cathepsin G and leukocyte elastase.

Inhibition of factor X$_a$. Fig. 3A shows the results obtained when factor X$_a$ is inhibited by full-length TFPI or the two different forms of truncated TFPI. Inhibition of factor X$_a$ by full-length TFPI was significantly stronger than that by TFPI-(1−247)-peptide. Inhibition by TFPI(1−247)-peptide was in turn stronger than that observed by TFPI-(1−161)-peptide. The results were analyzed in terms of tight-binding inhibition as described in Materials and Methods. The K_i values are listed in Table 1.

KPI domains 1, 2 and 3, expressed as separate recombinant proteins in yeast, were tested for their inhibitory activity towards factor X$_a$. The results are shown in Fig. 3B. Only KPI domain 2 inhibited factor X$_a$ with significant affinity. KPI domains 1 and 3 were non-inhibitory. However, affinity of KPI domain 2 for factor X$_a$ was orders of magnitude lower than that of multidomain derivatives of TFPI. This difference is demonstrated by the curve of factor X$_a$ inhibition by TFPI-(1−161)-peptide (Fig. 3B).

The properties of KPI domain 2 and TFPI-(1−161)-peptide were further analyzed by investigating the inhibition factor X$_a$ at various fixed concentrations of the oligopeptide substrate (data not shown). The results suggested that both TFPI derivatives act as competitive inhibitors of factor X$_a$. The inhibition constant (K_i = 90 nM) obtained with separately expressed KPI domain 2 was much weaker than that of TFPI-(1−161)-peptide (K_i = 0.5 nM). The value obtained for KPI domain 2 was in accordance with that (K_i = 0.1 μM) recently reported for KPI domain 2 expressed in *Escherichia coli* [31].

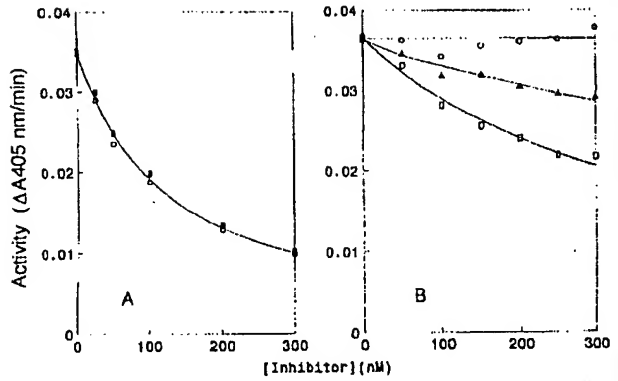

Fig. 4. Factor VII_a/TF inhibition by TFPI derivatives. (A) Full-length TFPI, (○); TFPI-(1−161)-peptide, (■). (B) KPI domain 1, (□); KPI domain 2, (▲); KPI domain 3, (○). Factor VII_a (10 nM) and TF (16 nM) were incubated in 50 mM Tris/Cl, 100 mM NaCl, 5 mM $CaCl_2$, 0.1% Tween 80, pH 7.4, with various concentrations of TFPI derivatives for 15 min. Substrate (0.6 mM Ile-Pro-Arg-NH-Np) was then added and residual activity measured.

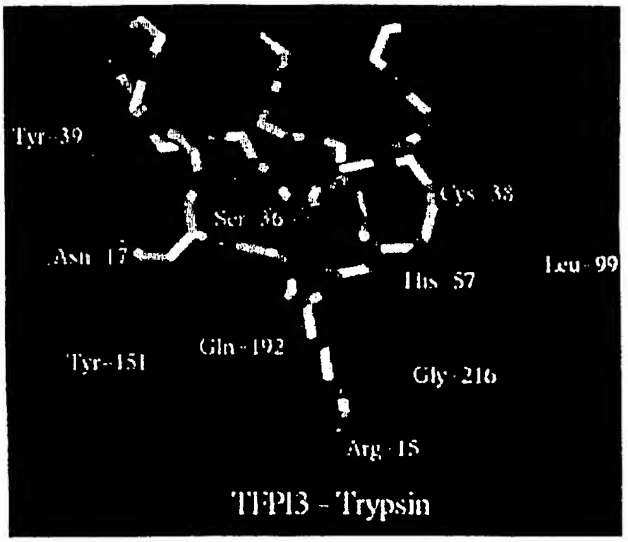

Fig. 5. Putative model of the complex betweeen TFPI-KPI domain 3 (TFPI3) and trypsin. The backbone of the TFPI-KPI-domain-3 loops comprising residues 10−20 and residues 33−40 are shown with the side chains of Cys14, Arg15, Asn17, Ser36 and Cys38. For clarity, only a few trypsin-residue side chains (Tyr39, His57, Leu99, Tyr151) and the backbone of Gly216 are shown in red. The unfavourably close contacts of trypsin residues His57 and Leu99 with the Cys14-Cys38 disulphide bridge of TFPI-KPI domain 3, which may block the inhibitory function of the molecule, are illustrated.

Inhibition of factor VII_a/TF. C-terminal truncation has a significant effect on inhibition of factor X_a by TFPI, but not of factor VII_a by TFPI. Fig. 4A shows the inhibition of factor VII_a by full-length TFPI and TFPI-(1−161)-peptide in the presence of TF-(1−218)-peptide. Similar results were obtained with detergent-solubilized full-length TF (data not shown). The inhibition constant (K_i = 0.12 μM) was higher than that previously published (K_i = 10 nM) which was obtained with relipidated full-length TF [12].

The inhibition of factor VII_a/TF by separate KPI domains is shown in Fig. 4B. KPI domain 3 was non-inhibitory, whereas KPI domain 1 inhibited (K_i = 0.25 μM) and KPI domain 2 weakly inhibited factor VII_a/TF (K_i = 1.1 μM).

DISCUSSION

TFPI contains three tandemly arranged KPI domains. The inhibition profile of each domain has been investigated in the present work. The three domains were found to have different properties which could not fully explain their functions as integrated parts of the intact TFPI molecule. A qualitative description of the interaction of the separate KPI domains with respective proteases at the molecular level is possible in terms of knowledge of the three-dimensional structure of these proteins. Molecular models can at least provide a description in terms of steric hindrance and electrostatic interactions.

TFPI-KPI domain 3. TFPI-KPI domain 3 seems to be non-inhibitory (Table 1). A plausible explanation for this finding is provided by a model (Fig. 5) based on the known structures of the KPI domain from α3 collagen type VI [26] and the KPI domain 2 from TFPI [24]. Fig. 5 shows the contact region of KPI domain 3 with the substrate-binding pocket of trypsin. We suggest that two features of the contact region of TFPI-KPI domain 3 contribute to preventing close interaction of this domain with serine proteases. The model indicates that Ser36 and the disulphide bond between Cys14 and Cys38 restrict the entry of the KPI domain into the substrate-binding pocket of trypsin. Position 36 is conserved as Gly in inhibitory KPI domains. Substitution of this Gly of BPTI with Ser resulted in profoundly decreased protease inhibition [34]. The authors suggested that this was due to changes in the stucture of the contact region of BPTI caused by displacement by the seryl side chain of an internal water molecule located close to Gly36, and to stabilization of the left-handed chirality of the Cys14−Cys38 disulphide bond, rather than the normal right-handed chirality. It has recently been demonstrated [26] that the non-inhibitory KPI domain from α3 collagen type VI attains the same left-handed chirality of its disulphide bond. We propose that in TFPI-KPI domain 3 the presence of Ser in position 36 and the absence of proline in its 10−14 backbone contribute to a twisted-loop conformation associated with stabilization of a left-handed disulphide-bond chirality. The model (Fig. 5) is based on the known structure of the KPI domain from α3 collagen type VI and the twist of the backbone loop of TFPI-KPI domain 3 is predicted to produce a 0.2-nm shift of the Sγ atom of Cys38 towards the enzyme. Steric hindrance between the Sγ atom of Cys38 and protease residues 57 and 99 restricts the entry of the KPI domain into the substrate-binding pocket of the serine proteases. In addition, the change in backbone conformation prevents the formation of a hydrogen bond between the carbonyl oxygen of residue 13 and the backbone nitrogen of residue 216 in the protease. The Asn in position 17 of domain 3, when inserted into the protease pocket, is placed in a small hydrophobic crevice formed by residues 38−41, 73, 74, 149−153, 192 and 193 of the protease. Direct hydrophobic contacts are possible with the protease residues 39 and 151. However, from the model it seems likely that the hydrophilic atoms of the Asn17 side chain are in unfavourably close contact with the hydrophobic atoms of the protease crevice. Similarly, residue 36 of TFPI-KPI domain 3 appears to collide with protease residue 192.

TFPI-KPI domain 2. The three-dimensional structure of TFPI domain 2 is known from X-ray studies [24], and a model of its complex with trypsin is shown in Fig. 6. A change in backbone conformation is induced by the presence of an aromatic (Tyr) side chain in position 17. A hydrogen bond seen in the BPTI ·

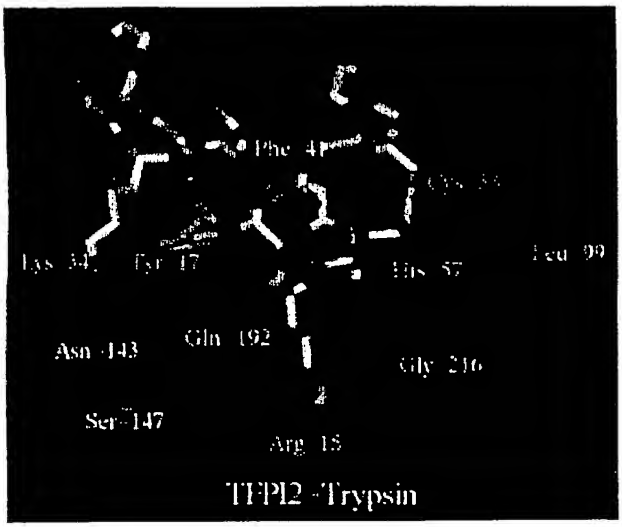

Fig. 6. Putative model of the complex betweeen TFPI-KPI domain 2 (TFPI2) and trypsin. The backbone of the TFPI-KPI-domain-2 loops comprising residues 10–20 and residues 33–40 and the side chains of Cys14, Arg15, Tyr17 and Cys38 are shown. Note the changed chirality of the Cys14–Cys38 disulphide chain and the changed backbone conformation of residues 16 and 17. For clarity, only a few trypsin-residue side chains (Phe41, His57, Leu99, Asn143, Ser147, Gln192) and the backbone of Gly216 are shown in red.

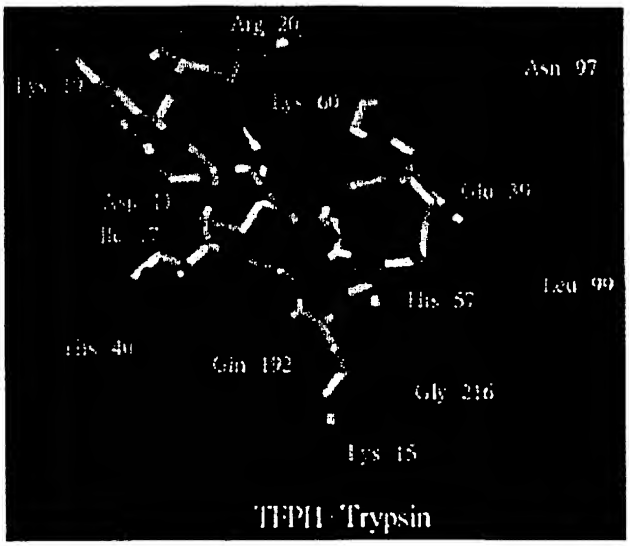

Fig. 7. Putative model of the complex betweeen TFPI-KPI domain 1 (TFPI1) and trypsin. The backbone of the TFPI-KPI-domain-1 loops comprising residues 10–20 and residues 33–40 are shown with the side chains of Asp11, Lys15, Ile17, Lys19, Arg20 and Glu39. For clarity, only a few trypsin-residue side chains (His40, His57, Lys60, Asn97, Leu99, Gln192) and the backbone of Gly216 are shown in red.

trypsin complex between the backbone nitrogen of inhibitor residue Ala17 and the backbone carbonyl of enzyme residue 41 is consequently lacking in complexes of TFPI-KPI domain 2 and trypsin. This conformational change also results in the Cα atom of Gly16 in TFPI-KPI domain 2 occupying the position of the Cβ atom of Ala16 in BPTI. Although the backbone conformation of the P′ region of TFPI-KPI domain 2 has been changed considerably compared with that observed in BPTI, the corresponding contact surface is similar to that of BPTI, and fits nicely into the substrate-binding pockets of various serine proteases. The contact region of TFPI-KPI domain 2 is therefore expected to be compatible with the substrate-binding cleft of a number of proteases, and to explain more subtle differences in the inhibition profile of this domain (Table 1), we have to look at residues in the vicinity of the substrate-binding cleft.

The main reason for the lack of inhibition of cathepsin G is ascribed to position Lys34 of TFPI-KPI domain 2. According to our model of cathepsin G (data not shown), Lys34 of the inhibitor would be in unfavourably close contact with a highly basic region on the surface of cathepsin G comprising Arg41, Arg143, Arg147 and Lys192. In factor X_a, residue 192 is a glutamine, whereas it is a lysine in factor VII_a. An electrostatic repulsion may partly account for the lower affinity of TFPI-KPI domain 2 for factor VII_a compared with factor X_a.

TFPI-KPI domain 1. In our model of TFPI-KPI domain 1 (Fig. 7) the scaffold is predicted to be similar in structure to that of the Alzheimer-amyloid-protein precursor KPI-domain [23]. Therefore, the backbone conformation of the reactive loop is similar to that in BPTI. However, TFPI-KPI domain 1 was a much weaker inhibitor than BPTI of trypsin and chymotrypsin. The weaker interaction of trypsin by domain 1 might be largely explained by the structure on the P′ side of the inhibitor. The side chain of residue 17 of the inhibitor has to fit into a small hydrophobic crevice in trypsin and the β-branched Ile17 side chain creates steric problems (Fig. 7). These steric problems apply particularly to the close contact between the Ile O′ oxygen and residue 151 of trypsin, but also one of the γ-carbon atoms of the side chain of residue 17 of the inhibitor gives rise to steric problems. Further, the basic inhibitor residues Lys19 and Arg20 might come in close contact with the enzyme residues Lys60 and Arg62. Thus the weak inhibition might be explained by a combination of steric hindrance and electrostatic repulsion. Similar arguments exist for chymotrypsin. The inhibitor residue Ile17 also creates steric problems for binding to this protease.

TFPI-KPI domain 1 inhibits cathepsin G but not factor X_a in contrast to TFPI-KPI domain 2. Putative models of the complex of domain 1 with factor X_a (data not shown) suggest that repulsion is created by Glu39 of the inhibitor, which is in very close contact with Glu97 of the protease. Cathepsin G inhibition by TFPI-KPI domain 1 is probably possible because of an electrostatic interaction between Asp11 of the inhibitor and Lys192 of the enzyme and because residue 34 (Ile) of the inhibitor is uncharged. Furthermore, the presence of a less bulky group in position 15 (Lys compared with Arg in TFPI-KPI domain 2) is likely to result in increased cathepsin G inhibition.

The stronger inhibition of factor VII_a by TFPI-KPI domain 1 compared with domain 2 is probably due to favourable interactions involving residues 34 (Ile) and 11 (Asp) of the inhibitor, which appear to interact with Lys341 of factor VII_a [35].

Additional secondary-site interactions. KPI domain 2 inhibits trypsin strongly (Table 1). The apparent K_i is similar to that obtained with derivatives of TFPI containing all three domains. The inhibition of trypsin by KPI domain 1 is 100-fold weaker than that by domain 2, and KPI domain 3 is non-inhibitory. The results suggest that inhibition of trypsin by TFPI is dominated by interactions with KPI domain 2. Secondary interactions with other regions appear to be of minor importance for trypsin inhibition. This is in contrast to inhibition of factor X_a by TFPI.

Previous studies [15–18] strongly indicated that KPI domain 2 of TFPI is involved in the interaction with factor X_a. This

interpretation is supported by the present study which shows that domain 2 is the only separately expressed TFPI domain with significant affinity for factor X_a. Interaction of the active-site region of factor X_a with a primary contact area on the KPI domain is pertinent to the inhibitory action of TFPI. However, it is clear that other regions contribute to the binding of TFPI and factor X_a. This is demonstrated by the 1000-fold higher affinity for factor X_a of intact full-length TFPI compared with the separate KPI domain 2.

Cleavage of TFPI between KPI domains 1 and 2 by elastase essentially abrogates the anti-factor X_a activity of TFPI [16, 17] further demonstrating the importance of an intact three-domain structure. A similar effect on the anti-factor X_a activity was observed upon cleavage of the two-domain inhibitor, TFPI-(1–161)-peptide (Petersen, L. C., unpuplished results). The results suggest an effect on factor X_a inhibition due to secondary interactions with the N-terminal part of TFPI. However, interactions with the C-terminal part of TFPI also affect the kinetics of inhibition as indicated by transient-inhibition experiments [36] showing that the rate constant for association of factor X_a with full-length TFPI ($k_{on} = 5.1 \times 10^6\ M^{-1}\ s^{-1}$) is fourfold faster than the reaction with the truncated derivative [TFPI-(1–247)-peptide].

In summary, the results of the present study indicate that the high affinity of intact TFPI for factor X_a arises as a consequence of interactions involving multiple segments of the inhibitor. Separation of the domains of TFPI leads to dramatically decreased affinity for factor X_a. Inhibition of proteases by KPI are generally thought to occur mainly as a result of an interaction between a suitable contact area on a rigid inhibitor scaffold and a substrate-binding pocket of a serine protease. Such interactions can be very strong as exemplified by the interaction between BPTI and trypsin, K_i of 0.06 pM [37]. By comparison the interaction between KPI domain 2 and factor X_a is weak, K_i of 0.1 μM (Table 1). Rather than optimization of such primary interactions evolution appears to have favored the development of secondary-site interactions for inhibition of factor X_a. In terms of regulatory control, secondary-site interaction could be greatly advantageous compared with sheer primary interaction, and this might be an important aspect of the molecular mechanism of TFPI inhibition.

We wish to thank Elke Gottfriedsen and Inge Skræpgaard for excellent technical assistance. Dr Per F. Nielsen is thanked for performing the PDMS measurements and Dr Mogens Christensen for amino-acid-composition analysis.

REFERENCES

1. Davie, E. W., Fujikawa, K. & Kisiel, W. (1991) *Biochemistry 30*, 10363–10370.
2. Rapaport, S. I. & Rao, L. V. M. (1992) *Arterioscler. Thromb. 12*, 111–121.
3. Pedersen, A. H., Lund-Hansen, T., Bisgaard-Frantzen, H., Olsen, F. & Petersen, L. C. (1989) *Biochemistry 28*, 9331–9336.
4. Nakagaki, T., Foster, D. C., Berkner, K. L. & Kisiel, W. (1991) *Biochemistry 30*, 10819–10824.
5. Radcliffe, R. & Nemerson, Y. (1976) *J. Biol. Chem. 251*, 4797–4802.
6. Masys, D. R., Bajaj, S. P. & Rappaport, S. I. (1982) *Blood 60*, 1143–1150.
7. Hjort, P. F. (1957) *Scand. J. Clin. Lab. Invest. 9 (Suppl. 27)*, 1–182.
8. Rapaport, S. I. (1989) *Blood 73*, 359–365.
9. Brooze, G. J. Jr, Girard, T. L. & Novotny, W. F. (1990) *Biochemistry 29*, 7539–7546.
10. Wunn, T. C., Kretzmer K. K., Girard, T. J., Miletich, J. P. & Broze, G. J. Jr (1988) *J. Biol. Chem. 263*, 6001–6004.
11. Girard, T. J., Warren, L. A., Novotny, W. F., Likert, K. M., Brown, S. G., Miletich, J. P. & Broze, G. J. Jr (1989) *Nature 338*, 518–520.
12. Pedersen, A. H., Nordfang, O., Norris, F., Wiberg, F. C., Christensen, P. M., Moeller, K. B., Meidahl-Pedersen, J., Beck, T. C., Norris, K., Hedner, U. & Kisiel, W. (1990) *J. Biol. Chem. 265*, 16786–16793.
13. Broze, G. J. Jr (1992) *Trends Cardiovasc. Med. 2*, 72–77.
14. Nordfang, O., Bjørn, S. E., Valentin, S., Nielsen, L. S., Wildgoose, P., Beck, T. C. & Hedner, U. (1991) *Biochemistry 30*, 10371–10376.
15. Wesselschmidt, R., Likert, K., Girard, T., Wun, T.-C. & Broze, G. J. Jr (1991) *Blood 78*, 2004–2010.
16. Higuchi, D. A., Wun, T.-C., Likert, K. & Broze, G. J. Jr (1992) *Blood 79*, 1712–1719.
17. Petersen, L. C., Bjørn, S. E. & Nordfang, O. (1992) *Thromb. Haemostasis 67*, 537–541.
18. Baugh, R. J. & Travis, J. (1976) *Biochemistry 15*, 836–843.
19. Hamamoto, T., Yamamoto, M., Nordfang, O., Petersen, J. G. L., Foster, D. & Kisiel, W. (1993) *J. Biol. Chem. 268*, 8704–8710.
20. Petersen, J. G. L., Meyn, G., Rasmussen, J. S., Petersen, J., Bjørn, S. E., Jonassen, I., Christiansen, L. & Nordfang, O. (1993) *J. Biol. Chem. 268*, 13344–13351.
21. Petersen, L. C., Bjørn, S. E., Norris, F., Norris, K. Sprecher, C. & Foster, D. C. (1994) *FEBS Lett. 338*, 53–57.
22. Morrison, J. F. & Walsh, C. T. (1988) *Adv. Enzymol. Relat. Areas Mol. Biol. 61*, 201–301.
23. Hynes, T. R., Randal, M., Kennedy, L. A., Eigenbrot, C. & Kasiakoff, A. A. (1990) *Biochemistry 29*, 10018–10022.
24. Birktoft, J. J., Norris, K. & Norris, F. (1993) *Thromb. Haemostasis 69*, 679.
25. Wlodawer, A., Deisenhofer, J. & Huber, R. (1987) *J. Mol. Biol. 193*, 145–156.
26. Arnoux, B., Ducruix, A., Norris, F., Norris, K. & Petersen, L. C. (1995) *J. Mol. Biol. 246*, 609–617
27. Otting, G. & Wüthrich, K. (1993) *Biochemistry 32*, 3571–3582.
28. Blevins, R. A. & Tulinsky, A. (1985) *J. Mol. Biol. 260*, 4264–4275.
29. Remington, S. J., Woodbury, R. G., Reynolds, R. A., Matthews, B. W. & Neurath, H. (1988) *Biochemistry 27*, 8097–8105.
30. Huber, R., Kukla, D., Bode, W., Schwager, P., Bartels, K., Deisenhofer, J. & Steigelmann (1974) *J. Mol. Biol. 89*, 73–101.
31. Day, K. C. & Welsch, D. J. (1992) *Thromb. Res. 68*, 369–381.
32. Zhou, J.-M., Liu, C. & Tsou, C.-L. (1989) *Biochemistry 28*, 1070–1076.
33. Broze, G. J. Jr, Warran, L. A., Novotny, W. F., Roesch, K. M. & Miletich, J. P. (1987) *Blood 71*, 385.
34. Berndt, K. D., Beunink, J., Schröder, W. & Wüthrich, K. (1993) *Biochemistry 32*, 4564–4570.
35. Wildgoose, P., Birktoft, J., Foster, D., Worsaae, H. Christensen, P. M. & Petersen, L. C. (1993) *Thromb. Haemostasis 69*, 957.
36. Lindhout, T., Willems, G., Blezer, R. & Hemker, C. (1994) *Biochem. J. 297*, 131–136.
37. Lazdunski, M., Vincent, J.-P., Schweitz, H., Peron-Renner, M. & Pudles, J. (1974) in *Proteinase inhibitors-Bayer symposium V* (Fritz, H., Tschesche, H., Greene, L. J. & Truscheit, E., eds) pp. 420–231, Springer-Verlag, Berlin.